CC Chemokine Ligand 18 in ANCA-Associated Crescentic GN

Silke R. Brix,* Gesa Stege,* Erik Disteldorf,* Elion Hoxha,* Christian Krebs,* Sonja Krohn,*
Benjamin Otto,[†] Kristin Klätschke,[†] Elisabeth Herden,* Felix Heymann,[‡] Sergio A. Lira,[§]
Frank Tacke,[‡] Gunter Wolf,[∥] Martin Busch,[∥] Wolfram J. Jabs,[¶] Fedai Özcan,**
Frieder Keller,[††] Joachim Beige,[‡‡] Karl Wagner,[§§] Udo Helmchen,[∥∥] Mercedes Noriega,[∥∥]
Thorsten Wiech,[∥∥] Ulf Panzer,* and Rolf A.K. Stahl*

*III. Medizinische Klinik and Institut für [†]Klinische Chemie and Institut für [∥∥]Pathologie, Universitätsklinikum Hamburg
Eppendorf, Hamburg, Germany; [‡]Medizinische Klinik III, Uniklinik Rheinisch Westfälische Technische Hochschule,
Aachen, Germany; [§]Immunology Institute, Icahn School of Medicine at Mount Sinai, New York, New York; [∥]Klinik für
Innere Medizin III, Universitätsklinikum Jena, Jena, Germany; [¶]Klinik für Innere Medizin, Vivantes Klinikum im
Friedrichshain, Berlin, Germany; **Klinik für Nephrologie und Notfallmedizin, Klinikum Dortmund, Dortmund,
Germany; [††]Abteilung Innere Medizin I, Universitätsklinikum Ulm, Ulm, Germany; [‡‡]Abteilung Nephrologie, Klinikum
St. Georg, Leipzig, Germany; and [§§]IV Medizinische Abteilung, Asklepios Klinik Barmbek, Hamburg, Germany

ABSTRACT

ANCA-associated vasculitis is the most frequent cause of crescentic GN. To define new molecular and/or cellular biomarkers of this disease in the kidney, we performed microarray analyses of renal biopsy samples from patients with ANCA-associated crescentic GN. Expression profiles were correlated with clinical data in a prospective study of patients with renal ANCA disease. CC chemokine ligand 18 (CCL18), acting through CC chemokine receptor 8 (CCR8) on mononuclear cells, was identified as the most upregulated chemotactic cytokine in patients with newly diagnosed ANCA-associated crescentic GN. Macrophages and myeloid dendritic cells in the kidney were detected as CCL18-producing cells. The density of CCL18^{+} cells correlated with crescent formation, interstitial inflammation, and impairment of renal function. CCL18 protein levels were higher in sera of patients with renal ANCA disease compared with those in sera of patients with other forms of crescentic GN. CCL18 serum levels were higher in patients who suffered from ANCA-associated renal relapses compared with those in patients who remained in remission. Using a murine model of crescentic GN, we explored the effects of the CCL18 murine functional analog CCL8 and its receptor CCR8 on kidney function and morphology. Compared with wild-type mice, $Ccr8^{-/-}$ mice had significantly less infiltration of pathogenic mononuclear phagocytes. Furthermore, $Ccr8^{-/-}$ mice maintained renal function better and had reduced renal tissue injury. In summary, our data indicate that CCL18 drives renal inflammation through CCR8-expressing cells and could serve as a biomarker for disease activity and renal relapse in ANCA-associated crescentic GN.

ANCA-associated vasculitis is the major cause of rapidly progressive GN. Despite substantial progress in our understanding of the pathophysiology of the disease, renal outcomes remain poor in a large percentage of patients.[1–7] In addition, renal survival has not improved significantly with the application of new therapeutic approaches.[8–11] Histopathologic features and the clinical course of the disease are variable, and assessment of disease activity is

often limited because of the lack of reliable disease-specific biomarkers.

To define new biomarkers of disease activity, we conducted a prospective study in patients with ANCA-associated crescentic GN by analyzing microarrays of renal biopsies from paraffin-embedded tissues. Among a large number of differentially expressed genes, CC chemokine ligand 18 (CCL18) was the most upregulated chemokine in patients with the disease compared with healthy controls. There is substantial evidence that chemokines and their receptors drive renal leukocyte recruitment and thereby, play an important role during the progression of ANCA-associated crescentic GN.[12] Therefore, we investigated whether CCL18 could be a marker for clinical disease activity.

Until recently, a rodent counterpart of human CCL18 had not been identified. In 2013, Islam *et al.*[13] reported the murine CCL8 (mCCL8) as its functional analog. Both chemokines acted through CC chemokine receptor 8 (CCR8) and were induced in alternatively activated macrophages[14–17] as well as in similar diseases.[18–20] Similar cytokine patterns regulated the induction of CCL18 and mCCL8.[13] Therefore, we aimed to investigate the functional role of CCR8 in crescentic GN by analyzing $Ccr8^{-/-}$ mice in an experimental model of murine crescentic GN.

Our results indicate that serum levels of CCL18 reflect the disease activity of ANCA-associated crescentic GN and therefore, might be used as a biomarker of this disease.

RESULTS

Patients with ANCA-Associated Crescentic GN
Ninety-six patients with a diagnosis of ANCA-associated crescentic GN were included in this study; 53 of these patients were proteinase 3 (PR3)-positive, and 43 of these patients were myeloperoxidase (MPO)-positive. The clinical baseline characteristics of the patients are summarized in Table 1. Blood samples were collected from 18 patients every 3 months for a period of 18 months (Figure 1).

Table 1. Clinical baseline characteristics of the patients

Clinical Characteristics	n (%)
Patients	96
Age at onset of symptoms	63.3±12.9[a]
Men	70 (73)
ANCA type	
PR3	53 (55)
MPO	43 (45)
Renal function at time of diagnosis	
Creatinine clearance[b]	34.9±24.5[c]
Dialysis dependence	26 (27)

[a]Years±SD.
[b]Patients not on dialysis.
[c]ml/min±SD.

Microarray Analysis Reveals CCL18 as the Most Upregulated Chemokine in ANCA-Associated Crescentic GN
Microarray analyses of renal biopsies were performed. A protocol for RNA isolation was established to obtain large amounts of intact RNA from formalin-fixed, paraffin-embedded (FFPE) samples. RNA of a very high quality was obtained (Supplemental Figure 1A).[21,22] RNA of sufficient quality for amplification and hybridization was obtained from 30 patients with ANCA-associated crescentic GN and 12 controls (pre-implantation kidney biopsies of living or deceased kidney donors). The patient characteristics and clinical data of the group of patients from whom RNA was isolated were not significantly different from those from the remaining patients included in the study (Supplemental Table 1). Biopsies of patients with renal ANCA disease displayed an upregulation of 1310 transcripts and a downregulation of 342 transcripts compared with control biopsies (signal log ratio≥1.0 or ≤−1.0; corrected $P<0.01$). Genes that were upregulated 7-fold or higher are shown in Figure 2A. Gene ontology annotation of biologic function showed a strong upregulation of transcripts associated with the immune response (Supplemental Figure 1B). Among these genes, *CCL18* was one of the most upregulated transcripts and the most upregulated chemokine in renal ANCA disease (Figure 2B). A 98-fold elevated expression of *CCL18* was validated by real-time PCR in 14 patients with ANCA-associated crescentic GN compared with 12 controls (biopsies of living and deceased kidney donors; $P<0.05$) (Figure 2C). A strong correlation between the expression of *CCL18* and other molecules involved in inflammation was observed (Supplemental Table 2).

Localization of CCL18- and CCR8-Expressing Cells in the Kidney by Immunohistochemical Analysis
To localize CCL18- and CCR8-expressing cells in the kidney, immunohistochemistry was performed in 31 renal biopsies of patients with ANCA-associated crescentic GN. CCL18^{+} cells were identified as infiltrating interstitial mononuclear cells (Figure 3, A and B). Consistent with their morphologic appearance, staining of consecutive sections with CCL18, CD68, and CD209 (dendritic cell [DC]-specific intracellular adhesion molecule-3–grabbing nonintegrin [SIGN]) revealed CCL18^{+} cells coexpressing CD68 as well as CCL18^{+} CD68^{+} cells coexpressing CD209 (Figure 3, C–E). A quantitative analysis identified 34.2%±6.6% of these cells as CCL18^{+} CD68^{+} and 17.0%±8.7% of these cells as CCL18^{+} CD68^{+} CD209^{+}. Staining of consecutive sections with CCL18, CD3, and CD20 did not reveal CCL18^{+} cells as CD3^{+} or CD20^{+} (data not shown). Immunohistochemistry of renal tissue sections derived from patients with ANCA-associated crescentic GN indicated that CCR8^{+} mononuclear cells obtain the characteristics of macrophages. Staining of consecutive sections showed single CD68^{+} cells coexpressing CCR8 (Figure 3, F and G). No coexpression of CCL18 and CCR8 was observed.
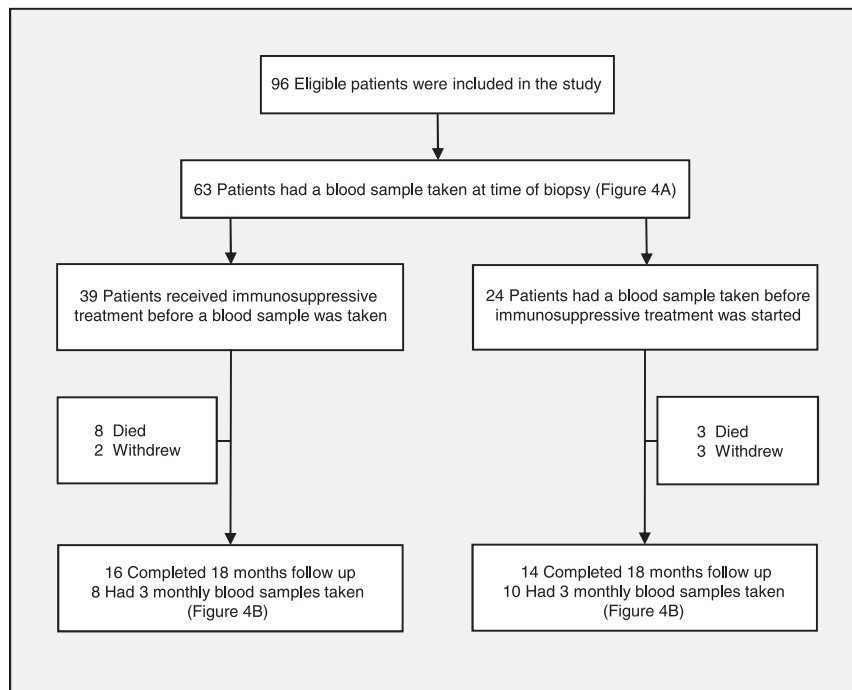
Figure 1. Flow chart shows the patients included in the study and their follow up. Ninety-six patients were included and blood samples were collected from 63 patients at the time of diagnosis. In 24 patients, a blood sample was collected before initiation of immunosuppression. A complete 3-monthly clinical follow-up was achieved in 30 patients, with the collection of an initial blood sample at the time of diagnosis.

Patient characteristics and clinical data did not differ significantly in the group of patients from whom biopsy specimens were analyzed for immunohistochemistry compared with the remaining patients included in the study (Supplemental Table 1).

CCL18$^+$ cells were observed predominantly in the inflamed, nonscarred tubulointerstitium. The cells were also found in atrophic tubulointerstitial areas and rarely, the glomeruli. In patients with renal ANCA disease, the density of CCL18$^+$ cells correlated with the mRNA levels of CCL18 ($P<0.01$) (Figure 3H). CCL18 mRNA levels correlated with the percentage of cellular crescents ($P<0.01$) (Figure 3I). The percentage of crescents, including cellular, fibrocellular, and sclerotic crescents, also correlated with the number of CCL18$^+$ cells ($P<0.05$) (Supplemental Figure 2A). The strongest correlation was found with cellular crescents only ($P<0.01$) (Figure 3J). Furthermore, the number of CCL18$^+$ cells correlated with the severity of the acute interstitial inflammation ($P<0.001$) (Figure 3K). The degree of interstitial fibrosis and tubular atrophy (Figure 3L) and the infiltration of T lymphocytes and macrophages did not correlate with the density of CCL18$^+$ cells (Supplemental Figure 2, B and C). The number of CCL18$^+$ cells correlated negatively with the GFR at the time of biopsy ($P<0.05$) (Figure 3M).

CCL18 Serum Levels Are Elevated in ANCA-Associated Crescentic GN
Serum CCL18 levels in patients with ANCA-associated crescentic GN were significantly higher than those of healthy volunteers and patients with non–ANCA-associated crescentic GN ($P<0.001$) (Figure 4A). CCL18 serum levels decreased during immunosuppressive treatment and remained low during follow-up ($P<0.05$) (Figure 4B). The decrease in CCL18 serum levels was even more pronounced when patients were excluded for requiring rescue therapy for disease activity during follow-up (Supplemental Figure 2D). Patients received standard induction therapy with steroids and cyclophosphamide or rituximab. Information on patient outcome is summarized in Figure 1 and Table 2.

CCL18 Serum Levels Are Elevated in Patients with Relapsing ANCA Disease
Renal relapse was determined as initiation of immunosuppressive rescue therapy because of clinical signs of renal disease activity. Renal disease activity was defined as rising serum creatinine and urinary red cell casts or a repeat biopsy with fresh ANCA-associated glomerular lesions. Eleven patients suffered from relapsing renal disease. These patients had higher CCL18 serum levels at the time of biopsy compared with patients who remained in remission during follow-up ($P<0.05$) (Figure 4C). In four of these patients, a CCL18 serum level was assessed at the onset of relapse (Figure 4, D–G).

CCL18 Serum Levels Do Not Correlate with Serum Levels of ANCA
Correlation analyses were performed between serum levels of CCL18, MPO, and PR3 at the time of study inclusion. Neither positive nor negative correlations were detected (Supplemental Figure 2, E and F). There were also no significant differences in the disease and antibody subgroups, between men and women, or in patients with involvement of other organs (*i.e.*, lung involvement) (Supplemental Figure 2, G–J).

CCR8 Drives the Recruitment of Pathogenic Mononuclear Phagocytes in Experimental Crescentic GN
We evaluated the role of mCCL8 and its receptor CCR8 in a murine model of crescentic GN (nephrotoxic nephritis [NTN]).

We analyzed mRNA expression levels during the course of disease. Quantitative RT-PCR of renal cortex samples showed that both CCR8 and CCL8 were highly upregulated (Figure 5A). CCL8 expression was markedly increased from day 5 onward (day 10: 116.5-fold versus the non-nephritic control). The CCR8 mRNA expression level showed a similar increase, with a peak at day 10 (4-fold versus the non-nephritic control). CCL1, the
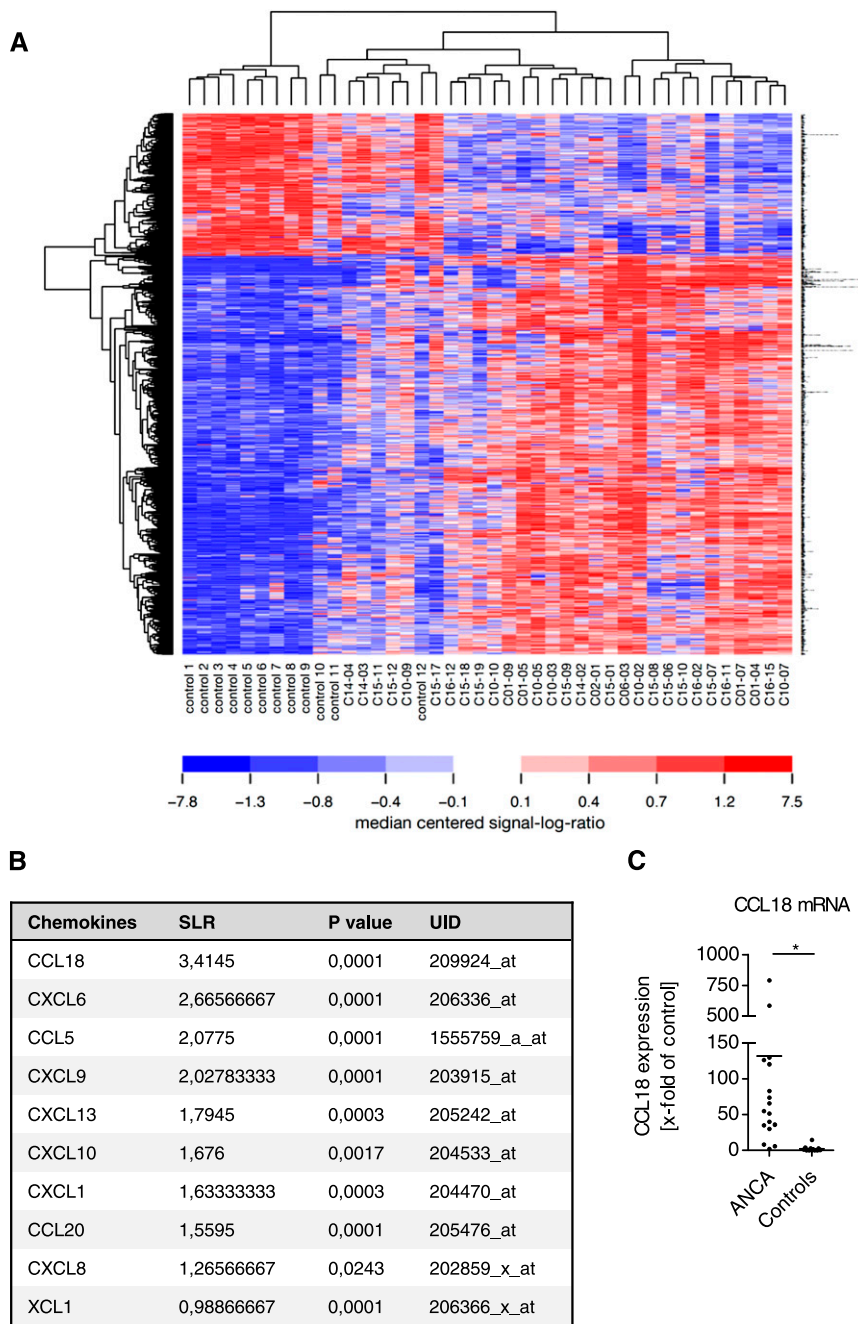
A

B

Chemokines	SLR	P value	UID
CCL18	3,4145	0,0001	209924_at
CXCL6	2,66566667	0,0001	206336_at
CCL5	2,0775	0,0001	1555759_a_at
CXCL9	2,02783333	0,0001	203915_at
CXCL13	1,7945	0,0003	205242_at
CXCL10	1,676	0,0017	204533_at
CXCL1	1,63333333	0,0003	204470_at
CCL20	1,5595	0,0001	205476_at
CXCL8	1,26566667	0,0243	202859_x_at
XCL1	0,98866667	0,0001	206366_x_at

C

CCL18 mRNA

Figure 2. Microarray analysis shows CCL18 as the highest upregulated transcript among all chemokines in ANCA-associated crescentic GN. (A) Heat map of differentially regulated transcripts in ANCA-associated crescentic GN compared with control kidneys. The RNA from 30 patients with ANCA-associated crescentic GN and 12 controls (preimplantation kidney biopsies of living or deceased kidney donors) was used for the microarray analyses. Total RNA was isolated from FFPE renal biopsies. Transcripts shown in this heat map had a signal log ratio≥2.3 and ≤−2.3 and were considered differentially expressed. Each column represents one biopsy sample, and each row shows the results for one probe set per transcript. Blue indicates downregulation of the probe sets, and red indicates upregulation of the probe sets. Areas in white represent no regulation. (B) Summary of the chemokines assessed. The unique identification number (UID) is indicated for each sample. A signal log ratio (SLR) of 3.41 was obtained for CCL18. (C) Quantitative real-time PCR analysis confirmed the high level of CCL18 expression. Total RNA from FFPE kidney biopsies was examined

previously known ligand of CCR8, was also upregulated in the inflamed renal cortex (41-fold versus the non-nephritic control at day 10) (Figure 5A).

Next, we investigated leukocyte infiltration in $Ccr8^{-/-}$ mice during crescentic GN. $Ccr8^{-/-}$ mice showed a markedly reduced infiltration of mononuclear phagocytes in the inflamed kidney compared with nephritic wild-type (WT) mice. Immunohistologic staining of F4/80, a glycoprotein expressed by interstitial mononuclear phagocytes,[23] revealed fewer F4/80-expressing cells in the inflamed renal tubulointerstitium in $Ccr8^{-/-}$ mice (38.5 cells/low-power field) compared with nephritic WT mice (46 cells/low-power field) (Figure 5, B and C). The renal flow cytometry analysis revealed a significantly reduced number of $CD11b^+$ $F4/80^+$ leukocytes in the nephritic renal cortex of $Ccr8^{-/-}$ mice (23% of $CD45^+$ $CD11b^+$ $F4/80^+$ leukocytes) compared with nephritic WT mice (30% of $CD45^+$ $CD11b^+$ $F4/80^+$ leukocytes; $P<0.05$) (Figure 5, D and E). In contrast, renal $CD3^+$ T cell infiltration and renal Th1, Th17, and Th2 responses were unaltered in nephritic $Ccr8^{-/-}$ mice (Supplemental Figure 3). Quantification of mouse anti-sheep IgG subclasses in the serum of nephritic WT, $Ccr8^{-/-}$, and non-nephritic WT control mice revealed an unchanged humoral immune response in $Ccr8^{-/-}$ mice (Supplemental Figure 4).

Mononuclear phagocytes within the inflamed kidney comprise a heterogeneous group of inflammatory and regulatory cells.[23] Therefore, we aimed to functionally characterize the significantly altered population of $CD11b^+$ $F4/80^+$ cells. Intracellular staining of the proinflammatory cytokine TNF-α was conducted in leukocytes isolated from nephritic WT kidneys (Figure 5F). $CD11b^+$ $F4/80^+$ cells had a greater capacity to produce TNF-α compared with the $CD45^+$ $CD11b^-$ $F4/80^-$ control

for CCL18 expression (Hs00268113_m1; Life Sciences) in relation to the levels of 18S RNA (Hs03928985_g1; Life Sciences). Renal CCL18 expression was 98 times higher in ANCA-associated crescentic GN ($n=14$) compared with controls ($n=12$). Bars represent means±SDs. *$P<0.05$.
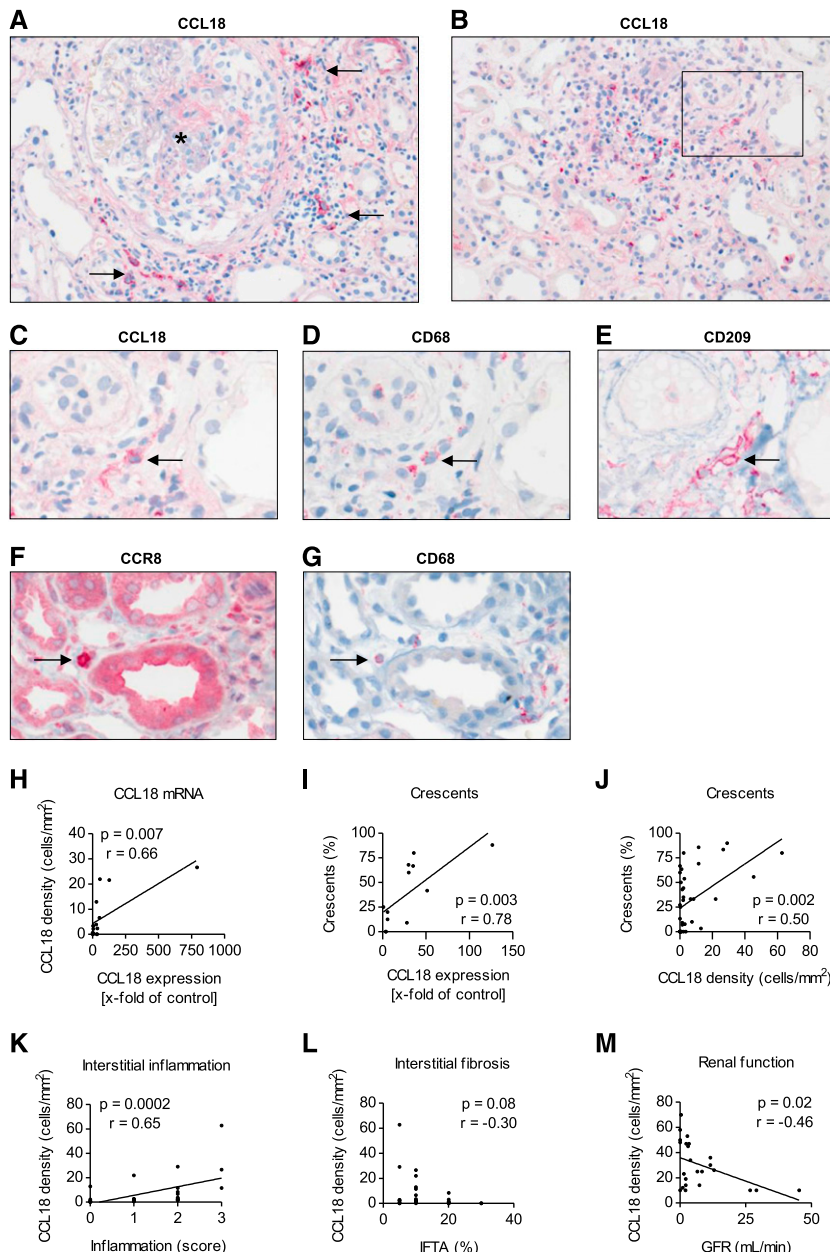
Figure 3. Immunohistochemistry reveals the presence of mononuclear intrarenal CCL18⁺ cells, which correlate with renal function at the time of biopsy. (A and B) Representative CCL18 immunohistochemistry of a renal biopsy from a patient with ANCA-associated crescentic GN showed that CCL18⁺ cells were predominantly located in the periglomerular and inflamed, nonscarred tubulointerstitium. Two-micrometer-thick FFPE tissue sections were stained for CCL18. Arrows indicate the CCL18⁺ cells surrounding a glomerulus marked with an asterisk (magnification, ×200). (C) CCL18, (D) CD68, and (E) CD209 staining revealed the presence of CCL18⁺ cells coexpressing CD68 and CD209. Arrows indicate a CCL18⁺ CD68⁺ CD209⁺ myeloid DC on the basis of staining of consecutive sections with CD68 and CD209 (original magnification, ×400). (F) Two-micrometer-thick FFPE tissue sections of patients with renal ANCA disease were stained for CCR8, identifying mononuclear CCR8⁺ cells with the appearance of macrophages. (G) Staining of consecutive sections with (F) CCR8 and (G) CD68 revealed the presence of CCR8⁺ cells coexpressing CD68 (original magnification, ×400). Arrows indicate a CCR8⁺ CD68⁺ macrophage on the basis of staining of consecutive sections with CD68. (H) The relative expression of CCL18

population, which suggested that these cells possessed a proinflammatory phenotype (Figure 5G).

CCR8 Promotes Renal Tissue Injury in Experimental Crescentic GN

NTN was induced in $Ccr8^{-/-}$ and WT mice. At day 8, $Ccr8^{-/-}$ mice showed significantly less tubulointerstitial and glomerular injury compared with control animals (Figure 6, A–C). The level of BUN was reduced in nephritic $Ccr8^{-/-}$ mice compared with nephritic WT mice at day 8 ($P<0.005$) (Figure 6D). Albuminuria was increased in both nephritic groups; however, there was no significant difference among the groups (Figure 6E).

Adoptively Transferred Monocytes Restore Kidney Injury in Nephritic $Ccr8^{-/-}$ Mice

Adoptive transfer was performed as previously described.[24] WT CD45⁺ CD115⁺ bone marrow-derived monocytes were adoptively transferred into WT or $Ccr8^{-/-}$ mice. NTN was induced after 24 hours, and the results were analyzed at day 8. Renal FACS analysis did not reveal differences in the quantification of CD11b⁺ F4/80⁺ mononuclear phagocytes between WT and $Ccr8^{-/-}$ mice (Figure 6, F and G). In addition, analysis of tubulointerstitial damage and glomerular injury revealed no differences in nephritic $Ccr8^{-/-}$ mice compared with nephritic mice (Figure 6, H and I).

DISCUSSION

Crescentic GN caused by ANCA-associated vasculitis is an aggressive and destructive

mRNA correlated with the density of CCL18⁺ cells ($n=15$). (I) The CCL18 mRNA levels correlated with the percentage of cellular crescents ($n=12$). (J) The percentage of cellular crescents correlated with the number of CCL18⁺ cells ($n=31$). (K) The density of CCL18⁺ cells correlated with the degree of acute interstitial inflammation ($n=31$). (L) The number of CCL18⁺ cells did not correlate with interstitial fibrosis and tubular atrophy (IFTA; $n=31$). (M) The density of the CCL18⁺ cells correlated with impairment of renal function (GFR) in patients who did not receive immunosuppressive treatment before renal biopsy ($n=24$).
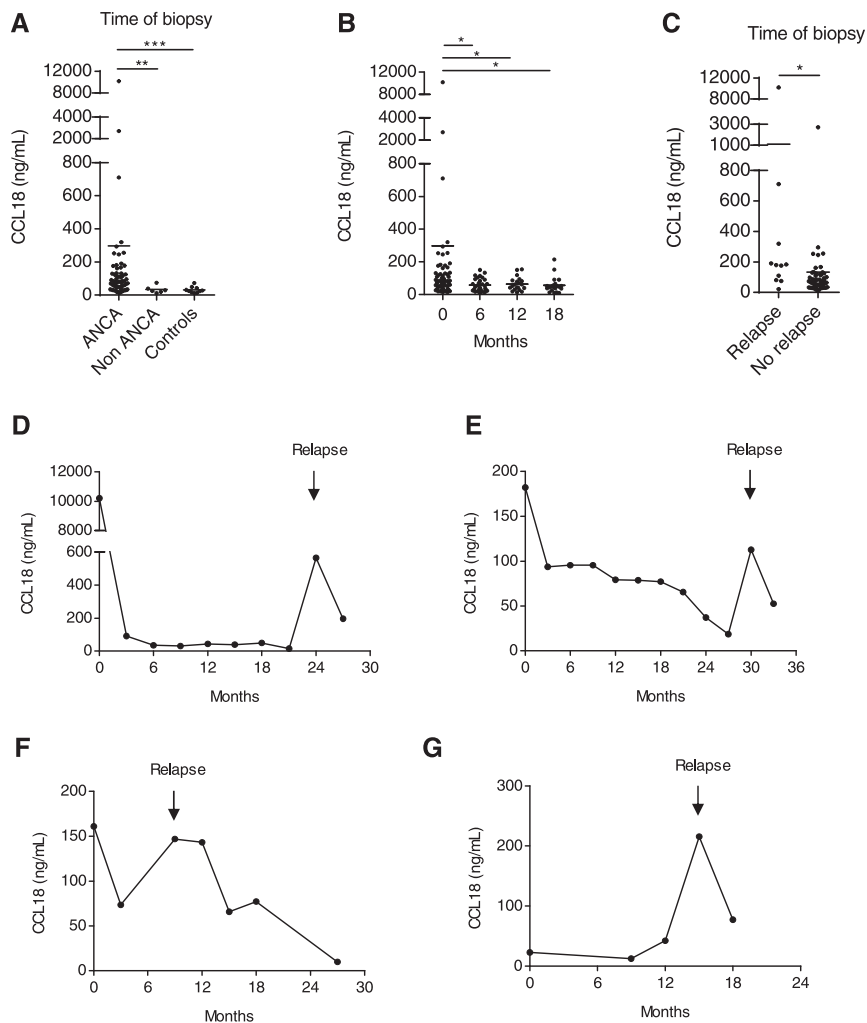
Figure 4. CCL18 serum levels are elevated in ANCA-associated crescentic GN. (A) CCL18 serum levels were compared among patients with ANCA-associated crescentic GN (ANCA GN), patients with non-ANCA GN, and healthy volunteers (controls). The levels of CCL18 were determined by ELISA. CCL18 serum levels were markedly elevated in patients with ANCA GN ($n=63$) compared with patients with non-ANCA GN ($n=6$) and healthy controls ($n=10$). CCL18 serum levels did not differ among patients with non-ANCA GN and healthy volunteers. (B) CCL18 serum levels were measured during follow-up. CCL18 serum levels decreased during the initial immunosuppressive treatment with cyclophosphamide or rituximab and remained low during the maintenance therapy with azathioprine. The CCL18 measurements obtained at the time of diagnosis ($n=63$) and 6 ($n=31$), 12 ($n=24$), and 18 months of follow-up are shown ($n=18$). (C) At the time of biopsy, CCL18 levels were significantly higher in patients who experienced a renal relapse during follow-up ($n=10$) compared with those who remained in remission ($n=53$). (D–G) Longitudinal study with serum measurements of CCL18 in patients suffering from renal relapsing disease. Arrows indicate the onset of relapse. Bars represent means±SDs. *$P<0.05$; **$P<0.01$; ***$P<0.001$.

disease that often causes end stage renal failure. Studies in rodent models and humans have shown that T cells, macrophages, and DCs play a central role in the development and progression of proliferative and crescentic GN.[23,25–33] Chemokines and their receptors have been identified as key regulators of directional leukocyte migration[12] and therefore,

might be an interesting therapeutic target or biomarker in patients with ANCA-associated crescentic GN.

Microarray analysis of kidney biopsies from patients with ANCA-associated crescentic GN revealed CCL18 as the most upregulated among all of the chemokine transcripts in renal tissues. CCL18 was originally detected in human fetal lung tissue and is mainly expressed by alternatively activated macrophages and DCs.[14,34,35] Enhanced CCL18 production together with elevated CCL18 serum levels have been reported in several inflammatory disorders and various cancers.[15,36] CCL18 has been proposed as a marker for disease activity[37] and shown to correlate with poor outcome in certain diseases.[37–40] Although some data indicate that CCL18 might act on immature DCs and T lymphocytes,[15,41–43] investigation of the biologic effects of CCL18 has been largely hampered by the lack of a known CCL18 receptor. The recent identification of CCR8 as the major receptor of CCL18 has permitted the functional evaluation of CCL18 and its murine analog CCL8.[13]

In our study, immunohistochemical analysis revealed the presence of CCL18 in intrarenal cells with a mononuclear appearance. Consecutive sections identified macrophages and myeloid DCs[25] coexpressing CCL18. The density of intrarenal CCL18+ cells correlated with the crescent formation, the degree of interstitial inflammation, and the impairment of renal function at the time of biopsy. Therefore, intrarenal mononuclear CCL18+ cells, which are present during acute inflammation and damage in ANCA-associated crescentic GN, might be either generated by or initiating and driving the disease process. This observation is supported by the strong correlation between CCL18 expression and the expression of other molecules involved in inflammation in renal tissue of patients with ANCA-associated crescentic GN. The number of myeloid DCs has been shown to correlate with increased serum creatinine in proliferative GN.[25] Consistently, the density of CCL18+ cells correlated with impairment of renal function in renal ANCA disease.

Because the density of CCL18+ cells in renal biopsies was associated with acute but not chronic kidney damage, we measured CCL18 serum levels to assess whether the chemokine levels correlated with disease activity or severity. CCL18 serum

Table 2. Clinical outcome of the patients after 18 months follow-up

Outcome	n (%)
ESRD	10 (10)
Renal relapse	11 (11)
Death	13 (14)

levels were significantly higher in patients with renal ANCA disease compared with patients suffering from non–ANCA-associated crescentic GN. CCL18 serum levels decreased during the 6 months of immunosuppressive induction treatment and remained low during follow-up, which indicated that CCL18 levels might reflect disease activity. Patients suffering from disease relapses had significantly higher CCL18 levels at the time of diagnosis. In four of these patients, CCL18 serum levels were assessed at onset of relapse and showed a rise at that time, further supporting this hypothesis. Therefore, CCL18 might serve as a marker of relapsing and persistent disease and might help to guide immunosuppressive treatment.

CCR8 has been recently discovered as a human receptor for CCL18.[13] This chemokine receptor is expressed on Th2 and regulatory T cells as well as on monocytes/macrophages.[44–47] We identified macrophages as CCR8-expressing cells in the kidneys of patients with renal ANCA disease as the renal target cell of CCL18. Immunohistochemistry did not reveal macrophages coexpressing CCL18 and CCR8, and we conclude that CCL18-producing cells and cells expressing CCR8 are two different cell populations.

Identification of CCR8 as a chemokine receptor for CCL18 as well as CCL8 as its murine analog enabled us to study the biologic function of this chemokine and its receptor in a murine model of crescentic GN. The model of NTN does not represent human renal ANCA disease in all aspects of its pathophysiology, but it is the most widely studied mouse model of crescentic GN. CCR8 and mCCL8 were upregulated in the kidneys of nephritic mice. Most importantly, nephritic $Ccr8^{-/-}$ mice had a reduced infiltration of renal mononuclear phagocytes and developed less severe crescentic GN with respect to renal function and renal tissue injury. The adoptive transfer study with $Ccr8^{-/-}$ mice receiving WT bone marrow-derived monocytes showed the importance of CCR8 for the renal mononuclear phagocyte infiltration. Because of the lack of male $Ccr8^{-/-}$ mice, we were not able to transfer CCR8$^{-/-}$ monocytes into nephritic CCR8$^{-/-}$ mice. Therefore, the explanatory power of the transfer experiment is limited, because it misses a control group.

In addition to CCL8, CCL1 (another ligand of CCR8) was found to be upregulated in nephritic kidneys of rodents. Despite that CCL1 upregulation was markedly inferior to CCL8 expression, we cannot claim an exclusive role for CCL8 in driving GN through CCR8 in mice. However, because CCL1 is not upregulated in human ANCA-associated crescentic GN, we highly assume that mCCL8 might reflect the target of interest in

rodents, which mimics best the effects that CCL18 drives during human GN.

Our data suggest that CCL18-secreting mononuclear cells might either attract monocytes by CCR8 and/or induce their differentiation into alternatively activated macrophages in renal ANCA disease. Through this mechanism, CCL18$^+$ cells could potentially be responsible for the acute cellular tissue inflammation in crescentic GN.

Our results indicate that the CCL18/CCR8 axis might play an important role in the recruitment of pathogenic mononuclear phagocytes in ANCA-associated crescentic GN. This hypothesis is on the basis of the upregulation of CCR8 as well as the murine CCL18 analog mCCL8 in experimental crescentic GN and the observation that $Ccr8^{-/-}$ mice display an ameliorated course of the disease. In summary, our data indicate that determination of the CCL18 level may support diagnosis and treatment decisions by clinicians for patients with ANCA-associated renal disease.

CONCISE METHODS

Study Design

The goal of this study was to define new molecular or cellular biomarkers in the kidney that indicate clinical outcomes in renal ANCA disease. In total, 96 patients with ANCA-associated crescentic GN with a diagnosis of granulomatosis with polyangiitis and microscopic polyangiitis were included in this prospective observational study. The non-ANCA GN control group comprised patients with a diagnosis of crescentic necrotizing GN caused by antiglomerular basement membrane disease (n=2), lupus (n=1), or IgA nephritis (n=3). Between March of 2009 and January of 2013, patients were recruited from 10 centers in Germany. Prospectively established inclusion criteria were as follows: (1) a rapid decline in renal function, (2) ANCA detected in the sera, and (3) necrotizing and crescentic GN in the kidney biopsy. The trial was performed in accordance with the Declaration of Helsinki. After informed consent was obtained, patient data, sera, and renal biopsies were collected according to the guidelines of the respective local ethics committees.

Data Collection

All of the patient data were collected prospectively, starting from the date of trial entry. Long-term follow-up data were acquired from a questionnaire filled in by physicians who participated in the trial. Additional necessary information concerning the patients' clinical status, renal function, infections, and other adverse events was obtained from discharge letters, including laboratory results and other electronically preserved documentation. The participating physicians performed disease assessments regularly every 3 months during the trial.

Entry Parameters

The baseline characteristics assessed were patient's age, sex, diagnosis, ANCA subtype, serum creatinine, eGFR, proteinuria, BP, and medication, including immunosuppressive treatment.
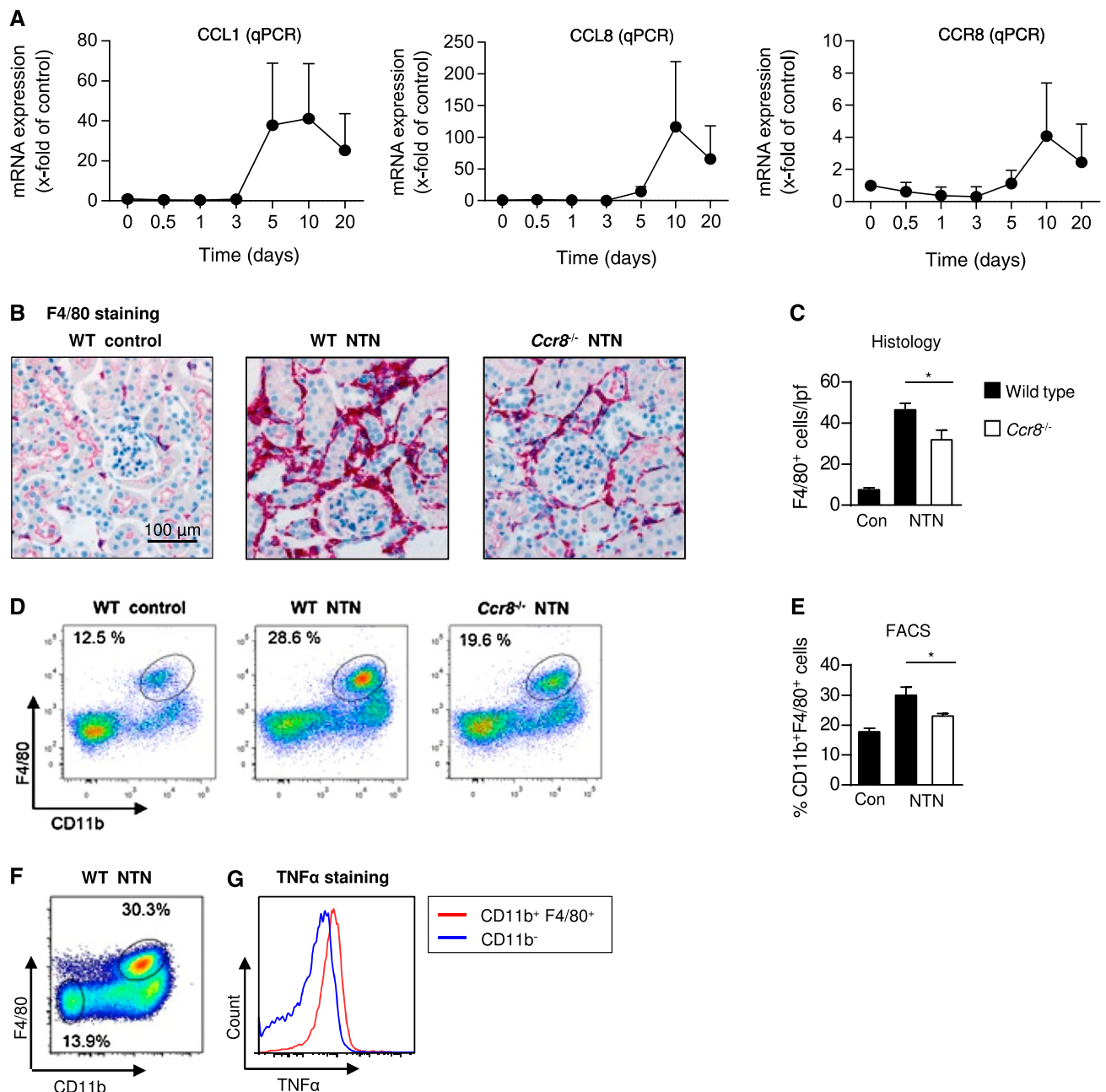
Figure 5. CCR8 drives the recruitment of pathogenic mononuclear phagocytes in crescentic GN. (A) RT-PCR analysis of renal CCL1, CCL8, and CCR8 mRNA expression during the course of nephritis ($n=5$–6). The mRNA expression is indicated as the x-fold change compared with non-nephritic WT controls. Symbols represent means±SDs. (B and C) Representative immunohistochemical photographs and quantification of renal tubulointerstitial leukocyte infiltration in nephritic WT, nephritic $Ccr8^{-/-}$, and WT control mice at day 8 after induction of nephritis using the macrophage marker F4/80 (magnification, ×200; WT control, $n=4$; nephritic WT and nephritic $Ccr8^{-/-}$, $n=9$). Bars represent means±SDs. (D) Representative FACS analysis of isolated renal leukocytes stained for the mononuclear phagocyte marker F4/80 from nephritic WT, $Ccr8^{-/-}$, and WT control mice at days 8 and 9 of nephritis. Plots were pregated on CD45$^+$, CD11b$^+$, and Ly6G$^-$ myelomonocytic leukocytes and are representative of three independent experiments. (E) Quantification of mononuclear phagocytes from the FACS analysis (WT control, $n=3$; nephritic WT and nephritic $Ccr8^{-/-}$, $n=5$). Bars represent means±SDs. (F) FACS analyses of renal CD11b$^+$ F4/80$^+$ cells isolated from controls and nephritic kidneys at day 8. Cells were pregated on CD45$^+$ leukocytes. Neutrophils were excluded from the analysis by negatively selecting for CD45$^+$, CD11b$^+$, and Ly6G$^+$ cells. Cells were restimulated with lipopolysaccharides and stained intracellularly for TNF-α. (G) The histogram shows TNF-α staining of CD11b$^+$ F4/80$^+$ cells or CD45$^+$ CD11b$^-$ cells as indicated. qPCR, quantitative PCR. *$P<0.05$.
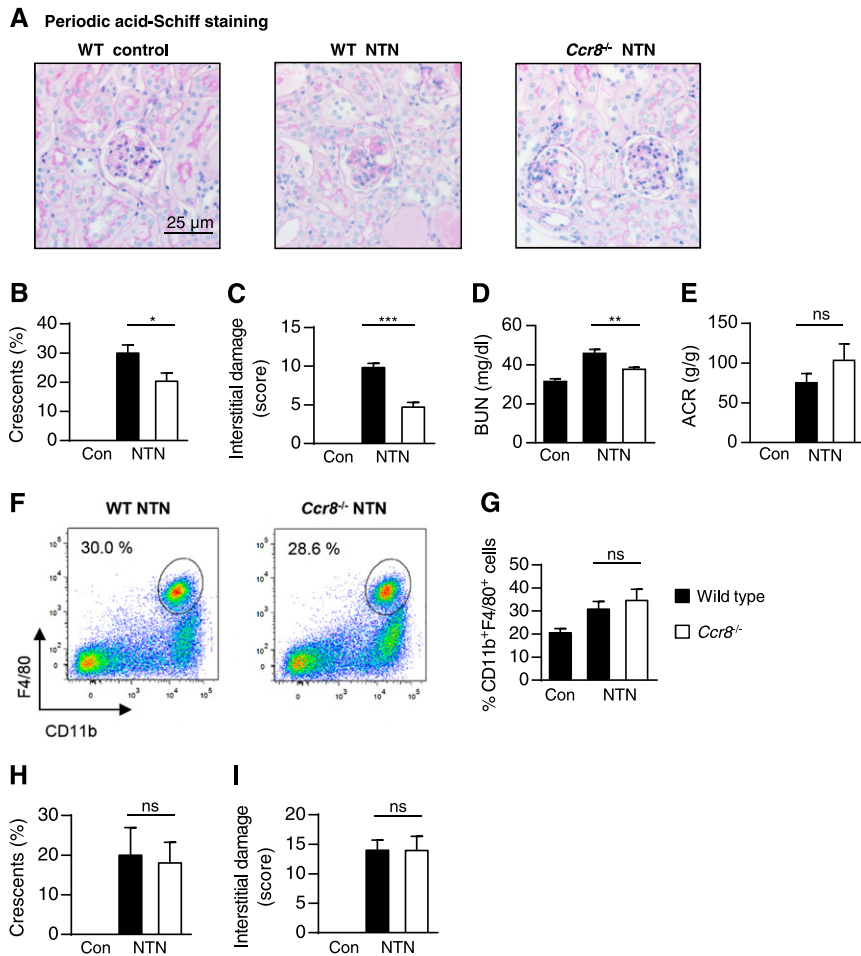
Figure 6. CCR8 drives renal tissue injury in experimental crescentic GN. (A) Representative photographs of periodic acid–Schiff-stained kidney sections of control, nephritic WT, and nephritic $Ccr8^{-/-}$ mice at day 8 after induction of nephritis (original magnifications, ×400 and ×200). Quantification of (B) glomerular crescent formation (WT control, n=9; nephritic WT and nephritic $Ccr8^{-/-}$, n=14), (C) tubulointerstitial damage (WT control, n=4; nephritic WT and nephritic $Ccr8^{-/-}$, n=5), and renal dysfunction assessed by determination of (D) BUN (WT control, n=9; nephritic WT and nephritic $Ccr8^{-/-}$, n=14) and (E) albuminuria (WT control, n=4; nephritic WT and nephritic $Ccr8^{-/-}$, n=9) at days 8 and 9 of nephritis in WT and $Ccr8^{-/-}$ mice (n=4–14). Bars represent means±SDs. (F) Representative FACS analysis of isolated renal leukocytes stained for the mononuclear phagocyte marker F4/80 from nephritic WT and $Ccr8^{-/-}$ mice, which received CD115$^+$ bone marrow-derived monocytes from nonnephritic WT mice at day −1 of nephritis. The analysis was performed at day 8 of nephritis. The plots were pregated on CD45$^+$, CD11b$^+$, and Ly6G$^-$ myelomonocytic leukocytes and are representative of three independent experiments. (G) Quantification of mononuclear phagocytes from the FACS analysis (n=6–7), with bars representing means±SDs. (H and I) Quantification of glomerular crescent formation and tubulointerstitial damage at day 8 of nephritis in WT and $Ccr8^{-/-}$ mice, which received WT CD115$^+$ bone marrow-derived monocytes (n=6–7). Bars represent means +SDs. Con, control. *$P<0.05$; **$P<0.01$; ***$P<0.001$.

Renal Biopsy Samples

In total, 30 biopsies from patients with ANCA-associated crescentic GN and 12 preimplantation biopsies from kidneys of healthy living and deceased renal donors were processed and used for microarray and real-time PCR analyses.

Isolation of RNA and cDNA Amplification

Total RNA was isolated from five 8-μm-thick sections of FFPE kidney biopsies using the High Pure FFPE RNA Micro Kit (Roche; Deutschland Holding GmbH, Grenzach-Wyhlen, Germany) with a modified protocol (Supplemental Material).[48] The RNA concentration was determined using a NanoDrop spectrophotometer, and the RNA quality was controlled using an Agilent Bioanalyzer. Fifty nanograms nondegraded RNA (Supplemental Material) was used as a template for reverse transcription. The WT-Ovation FFPE RNA Amplification System V2 (NuGEN, Leek, The Netherlands) was used for cDNA amplification according to the manufacturer's instructions.

Microarray Analyses

Fragmentation and labeling of amplified cDNA was performed using the Encore Biotin Module (NuGEN) according to the manufacturer's instructions. Four micrograms labeled cDNA was used to prepare the hybridization mix (Affymetrix, High Wycombe, UK). Samples were hybridized to Affymetrix U133 Plus 2.0 (Affymetrix) microarrays for 17 hours. Fragmentation, labeling, and hybridization were performed according to the protocol provided by the Encore Biotin Module (NuGEN). The data were published in the ArrayExpress database under accession number E-MTAB-1944.

Real-Time RT-PCR Analyses

Total RNA derived from kidney biopsies was used as a template for reverse transcription. The reaction was performed using 0.1 μg RNA, 100 ng/μl random hexamer primer (Invitrogen, Darmstadt, Germany), 10 mmol/L deoxyribonucleotide triphosphates (Invitrogen), and 200 units RevertAid Reverse Transcription (Fermentas GmbH, St. Leon-Rot, Germany). For cDNA synthesis, RNA and primer were incubated for 5 minutes at 65°C. Next, a 15 μl mixture of enzyme, buffer, and deoxyribonucleotide triphosphate was added to the RNA and primer to a final volume of 20 μl. The samples were incubated for 10 minutes at 25°C, 60 minutes at 42°C, and 10 minutes at 70°C. The real-time PCR reaction was performed using the Step One Plus Real-Time PCR System (Applied Biosystems, Foster City, CA) and validated primer pairs for CCL18 (Hs00268113_m1; Life Sciences). The assay was performed in triplicate. The expression of the CCL18 transcripts was quantified against the housekeeping gene 18S ribosomal

RNA (Hs03928985_g1; Life Sciences) using validated primer pairs. Real-time PCR was performed according to the protocol provided by the manufacturer. Total RNA was prepared according to standard laboratory methods. Real-time PCR was performed in a Step One Plus Real-Time PCR System (Applied Biosystems). All of the samples were run in duplicate and normalized to 18S ribosomal RNA to account for small variabilities in RNA and cDNA content.

ELISAs
Serum samples were collected at the time of biopsy and then every 3 months. Blood samples, which were used as controls, were collected one time after informed consent was obtained. Serum levels of CCL18 (DY394; R&D Systems, Abingdon, UK), anti-MPO antibodies (ORG 519; Orgentec, Mainz, Germany), and anti-PR3 antibodies (ORG 618; Orgentec) were determined by ELISA according to the protocol provided by the manufacturers, with slight modifications for the CCL18 ELISA (Supplemental Material).

Immunohistochemistry
The FFPE tissue sections were stained for CCL18, CD68, DC-SIGN, CCR8, CD3, and CD20. For CCL18 (500-P108; Preprotech) and CD68 (M 0814; Dako, Glostrup, Denmark), the sections were pretreated with a protease solution for 15 minutes at 37°C. For DC-SIGN (yDCN46; BD Biosciences Pharmigen, San Diego, CA), sections were treated in 0.1 M citrate buffer to retrieve antigen. CCR8 (NLS3847; Novus Biologicals, Littleton, CO) staining was performed after treatment in 0.1 M buffer solution to retrieve antigen (S1699; Dako) at pH 6. The sections were incubated with anti-CCL18 (1:200) and anti-CD68 (1:400) antibodies overnight at 4°C. Sections stained with anti–DC-SIGN (1:500), and anti-CCR8 (1:500) antibodies were incubated for 30 minutes at 37°C. Sections stained for CCL18, DC-SIGN, and CCR8 were developed using the POLAP-AP (Zytomed, Berlin, Germany). To detect CD68 staining, ABC-AP (Vector Laboratories, Burlingame, CA) was used. Staining of consecutive sections was performed, because double staining immunohistochemistry was technically not feasible because of different pretreatments of antibodies.

Histopathologic Evaluations
Periodic acid–Schiff and Giemsa staining were applied for renal histopathologic evaluations using light microscopy. Slides were examined by a nephropathologist who was blinded to the patient's data and research results. The degree of interstitial fibrosis and tubular atrophy was assessed. To further determine the inflammatory infiltrate, the interstitial inflammation was estimated analog to the BANFF classification.[49]

Animals
$Ccr8^{-/-}$ mice were generated by Chensue et al.[50] These mice displayed an aberrant T helper type 2 cell response and impaired eosinophil recruitment in vivo.[50] All of the mice were raised under specific pathogen-free conditions. Animal experiments were performed according to national and institutional animal care and ethical guidelines and approved by local ethics committees.

Induction of Crescentic GN (NTN) and Functional Studies
NTN was induced in 8- to 10-week-old male C57BL/6 WT or gene-deficient mice by intraperitoneal injection of 0.5 ml nephrotoxic sheep serum per mouse as previously described.[51] For urine sample collection, mice were housed in metabolic cages for 6 hours. Urinary albumin excretion was determined by standard ELISA analysis (Mice-Albumin Kit; Bethyl, Montgomery, TX), whereas urinary creatinine and BUN were measured using standard laboratory methods.

Murine Morphologic Analyses
Light microscopy and immunohistochemistry were performed using routine methods. Crescent formation was assessed in 50 glomeruli per mouse in a blinded fashion in periodic acid–Schiff-stained paraffin sections. As a measure for tubulointerstitial injury, the interstitial area was estimated by point counting of four independent areas of renal cortex per mouse under low magnification ($\times 200$) as previously described.[52] Two-μm-thick paraffin-embedded sections were stained with antibodies against the monocyte/macrophage cell markers F4/80 (BM8; BMA) and MAC-2 (M3/38; Cedarlane, Burlington, ON, Canada), the T cell marker CD3 (A0452; Dako), or sheep IgG (Jackson ImmunoResearch Laboratories) and mouse IgG (Jackson ImmunoResearch Laboratories). Tissue sections were developed using the Vectastain ABC-AP Kit (Vector Laboratories). MAC-2$^+$ and CD3$^+$ cells in 30 glomerular cross-sections as well as F4/80$^+$ and CD3$^+$ cells in 30 tubulointerstitial high-power fields (magnification, $\times 400$) were counted per kidney in a blinded manner using light microscopy. Glomerular deposition of mouse IgG and sheep IgG was scored from zero to three in 30 glomeruli per mouse.

Isolation of Leukocytes from the Kidney and Spleen
For leukocyte isolation from murine kidneys, we used previously described methods.[51] In brief, kidneys were finely minced and digested for 45 minutes at 37°C with 0.4 mg/ml collagenase D (Roche, Mannheim, Germany) supplemented with 10% heat-inactivated FCS (Invitrogen). Spleens were minced for the splenocyte isolation. Both cell suspensions were sequentially filtered through 70- and 40-μm nylon meshes and washed in HBSS without Ca^{2+} and Mg^{2+} (Invitrogen). Single-cell suspensions were separated using Percoll density gradient (70% and 40%) centrifugation. The leukocyte-enriched cell suspension was aspirated from the Percoll interface. After the erythrocytes had been removed using lysis solution (139 mM NH_4Cl and 19 mM Tris), cells were washed with HBSS and resuspended in FCS-containing buffer. Cell viability was assessed by trypan blue staining before flow cytometry or cell transfer experiments.

Flow Cytometry
For FACS analysis, renal leukocyte suspensions were stained for 20 minutes at 4°C with the following fluorochrome-conjugated antibodies: CD45 (30-F11), CD11b (M1/70), CD11c (HL3), F4/80 (BM8), CD3 (506A2), and CD4 (GK1.5; BD Biosciences, Franklin Lakes, NJ; eBioscience, San Diego, CA; or R&D Systems, Minneapolis, MN). Staining of intracellular TNF-α (MP6-XT22; BioLegend, San Diego, CA), IL-17A (TC11–18H10.1; BioLegend), IL-4 (11B11; Santa Cruz Biotechnology, Heidelberg, Germany), and IFN-γ (XMG1.2;

eBioscience) was performed as previously described.[53] In brief, cells were activated by incubation at 37°C with 5% CO_2 for 4 hours with phorbol 12-myristate 13-acetate (50 ng/ml; Sigma-Aldrich, St. Louis, MO) and ionomycin (1 μg/ml; Calbiochem-Merck, Darmstadt, Germany) or 1 μg/ml lipopolysaccharide (only for intracellular TNF-α staining) in X-VIVO medium (Lonza AG, Walkersville, MD). After a 30-minute incubation, Brefeldin A (10 μg/ml; Sigma-Aldrich) was added. Dead cells were stained (LIVE/DEAD Fixable Read Dead Stain Kit; Invitrogen), and samples were acquired using a Becton & Dickinson LSRII System with Diva software. Data analysis was performed using Flow Jo software (Tree Star Inc., Ashland, OR).

Adoptive Monocyte Transfer

For the adoptive monocyte transfer, previously described methods were used.[54] In brief, monocytes were purified from mouse bone marrow by immunomagnetic selection of CD115$^+$ cells using a CD115 biotin (BD Biosciences) antibody followed by a streptavidin magnetic assisted cell sorting conjugate (Miltenyi Biotec). The purity of the isolated monocytes was checked by flow cytometry and found to be 82.4%. Intravenous injection of 1.5×10^6 cells into WT and $Ccr8^{-/-}$ recipients was performed 24 hours before induction of NTN. Mice were euthanized after 8 days.

Assessment of Humoral Nephritogenic Immune Responses

Mouse anti-sheep IgG antibody titers were measured by ELISA using sera collected 10 days after induction of nephritis as previously described.[51] IgM and IgG titers were measured using the Ready-Set-Go ELISA according to the manufacturer's instructions (Bioscience, San Diego, CA).

Statistical Analyses

Microarrays were background-corrected and normalized using the Robust Multi-array Average procedure and quantile normalization, respectively.[55,56] The results were corrected for multiple testing using the bootstrapping procedure. A signal log ratio≥1.0 or ≤−1.0 and a corrected $P<0.01$ were considered to indicate statistical significance. Differences between two groups were compared using a two-tailed t test. In the case of multiple comparisons, one-way ANOVA with Bonferroni multiple comparisons test was performed using Graph-Pad Prism software. Comparison of CCL18 serum levels from patients with ANCA-associated crescentic GN and controls as well as the time course of CCL18 serum levels were conducted using the Kruskal–Wallis test. Correlation analyses of CCL18 serum levels and the density of CCL18$^+$ cells were performed using Spearman's rank correlation. $P<0.05$ was considered statistically significant.

ACKNOWLEDGMENTS

DISCLOSURES

None.

REFERENCES

1. Furuta S, Jayne DR: Antineutrophil cytoplasm antibody-associated vasculitis: Recent developments. *Kidney Int* 84: 244–249, 2013

2. Falk RJ, Jennette JC: Anti-neutrophil cytoplasmic autoantibodies with specificity for myeloperoxidase in patients with systemic vasculitis and idiopathic necrotizing and crescentic glomerulonephritis. *N Engl J Med* 318: 1651–1657, 1988

3. Falk RJ, Jennette JC: ANCA disease: Where is this field heading? *J Am Soc Nephrol* 21: 745–752, 2010

4. Kallenberg CG: Pathogenesis of ANCA-associated vasculitides. *Ann Rheum Dis* 70[Suppl 1]: i59–i63, 2011

5. Kain R, Exner M, Brandes R, Ziebermayr R, Cunningham D, Alderson CA, Davidovits A, Raab I, Jahn R, Ashour O, Spitzauer S, Sunder-Plassmann G, Fukuda M, Klemm P, Rees AJ, Kerjaschki D: Molecular mimicry in pauci-immune focal necrotizing glomerulonephritis. *Nat Med* 14: 1088–1096, 2008

6. Kain R, Tadema H, McKinney EF, Benharkou A, Brandes R, Peschel A, Hubert V, Feenstra T, Sengölge G, Stegeman C, Heeringa P, Lyons PA, Smith KG, Kallenberg C, Rees AJ: High prevalence of autoantibodies to hLAMP-2 in anti-neutrophil cytoplasmic antibody-associated vasculitis. *J Am Soc Nephrol* 23: 556–566, 2012

7. Jennette JC, Xiao H, Falk RJ: Pathogenesis of vascular inflammation by anti-neutrophil cytoplasmic antibodies. *J Am Soc Nephrol* 17: 1235–1242, 2006

8. Jones RB, Tervaert JW, Hauser T, Luqmani R, Morgan MD, Peh CA, Savage CO, Segelmark M, Tesar V, van Paassen P, Walsh D, Walsh M, Westman K, Jayne DR; European Vasculitis Study Group: Rituximab versus cyclophosphamide in ANCA-associated renal vasculitis. *N Engl J Med* 363: 211–220, 2010

9. Stone JH, Merkel PA, Spiera R, Seo P, Langford CA, Hoffman GS, Kallenberg CG, St. Clair EW, Turkiewicz A, Tchao NK, Webber L, Ding L, Sejismundo LP, Mieras K, Weitzenkamp D, Ikle D, Seyfert-Margolis V, Mueller M, Brunetta P, Allen NB, Fervenza FC, Geetha D, Keogh KA, Kissin EY, Monach PA, Peikert T, Stegeman C, Ytterberg SR, Specks U; RAVE-ITN Research Group: Rituximab versus cyclophosphamide for ANCA-associated vasculitis. *N Engl J Med* 363: 221–232, 2010

10. Specks U, Merkel PA, Seo P, Spiera R, Langford CA, Hoffman GS, Kallenberg CG, St. Clair EW, Fessler BJ, Ding L, Viviano L, Tchao NK, Phippard DJ, Asare AL, Lim N, Ikle D, Jepson B, Brunetta P, Allen NB, Fervenza FC, Geetha D, Keogh K, Kissin EY, Monach PA, Peikert T, Stegeman C, Ytterberg SR, Mueller M, Sejismundo LP, Mieras K, Stone JH; RAVE-ITN Research Group: Efficacy of remission-induction regimens for ANCA-associated vasculitis. *N Engl J Med* 369: 417–427, 2013

11. Schönermarck U, Gross WL, de Groot K: Treatment of ANCA-associated vasculitis. *Nat Rev Nephrol* 10: 25–36, 2014

12. Chung AC, Lan HY: Chemokines in renal injury. *J Am Soc Nephrol* 22: 802–809, 2011

13. Islam SA, Ling MF, Leung J, Shreffler WG, Luster AD: Identification of human CCR8 as a CCL18 receptor. *J Exp Med* 210: 1889–1898, 2013

14. Kodelja V, Müller C, Politz O, Hakij N, Orfanos CE, Goerdt S: Alternative macrophage activation-associated CC-chemokine-1, a novel structural homologue of macrophage inflammatory protein-1 alpha with a Th2-associated expression pattern. *J Immunol* 160: 1411–1418, 1998

15. Schutyser E, Richmond A, Van Damme J: Involvement of CC chemokine ligand 18 (CCL18) in normal and pathological processes. *J Leukoc Biol* 78: 14–26, 2005

16. Thomas GD, Rückerl D, Maskrey BH, Whitfield PD, Blaxter ML, Allen JE: The biology of nematode- and IL4Rα-dependent murine macrophage polarization in vivo as defined by RNA-Seq and targeted lipidomics. *Blood* 120: e93–e104, 2012

17. Egawa M, Mukai K, Yoshikawa S, Iki M, Mukaida N, Kawano Y, Minegishi Y, Karasuyama H: Inflammatory monocytes recruited to allergic skin acquire an anti-inflammatory M2 phenotype via basophil-derived interleukin-4. *Immunity* 38: 570–580, 2013

18. Islam SA, Chang DS, Colvin RA, Byrne MH, McCully ML, Moser B, Lira SA, Charo IF, Luster AD: Mouse CCL8, a CCR8 agonist, promotes atopic dermatitis by recruiting IL-5+ T(H)2 cells. *Nat Immunol* 12: 167–177, 2011

19. Prasse A, Pechkovsky DV, Toews GB, Schäfer M, Eggeling S, Ludwig C, Germann M, Kollert F, Zissel G, Müller-Quernheim J: CCL18 as an indicator of pulmonary fibrotic activity in idiopathic interstitial pneumonias and systemic sclerosis. *Arthritis Rheum* 56: 1685–1693, 2007

20. Liu T, Baek HA, Yu H, Lee HJ, Park BH, Ullenbruch M, Liu J, Nakashima T, Choi YY, Wu GD, Chung MJ, Phan SH: FIZZ2/RELM-β induction and role in pulmonary fibrosis. *J Immunol* 187: 450–461, 2011

21. Ribeiro-Silva A, Zhang H, Jeffrey SS: RNA extraction from ten year old formalin-fixed paraffin-embedded breast cancer samples: A comparison of column purification and magnetic bead-based technologies. *BMC Mol Biol* 8: 118, 2007

22. Hodgin JB, Borczuk AC, Nasr SH, Markowitz GS, Nair V, Martini S, Eichinger F, Vining C, Berthier CC, Kretzler M, D'Agati VD: A molecular profile of focal segmental glomerulosclerosis from formalin-fixed, paraffin-embedded tissue. *Am J Pathol* 177: 1674–1686, 2010

23. Nelson PJ, Rees AJ, Griffin MD, Hughes J, Kurts C, Duffield J: The renal mononuclear phagocytic system. *J Am Soc Nephrol* 23: 194–203, 2012

24. Tacke F, Yoneyama H: From NAFLD to NASH to fibrosis to HCC: Role of dendritic cell populations in the liver. *Hepatology* 58: 494–496, 2013

25. Segerer S, Heller F, Lindenmeyer MT, Schmid H, Cohen CD, Draganovici D, Mandelbaum J, Nelson PJ, Gröne HJ, Gröne EF, Figel AM, Nössner E, Schlöndorff D: Compartment specific expression of dendritic cell markers in human glomerulonephritis. *Kidney Int* 74: 37–46, 2008

26. Kurts C, Panzer U, Anders HJ, Rees AJ: The immune system and kidney disease: Basic concepts and clinical implications. *Nat Rev Immunol* 13: 738–753, 2013

27. Berden AE, Jones RB, Erasmus DD, Walsh M, Noël LH, Ferrario F, Waldherr R, Bruijn JA, Jayne DR, Bajema IM; European Vasculitis Society: Tubular lesions predict renal outcome in antineutrophil cytoplasmic antibody-associated glomerulonephritis after rituximab therapy. *J Am Soc Nephrol* 23: 313–321, 2012

28. Weidner S, Carl M, Riess R, Rupprecht HD: Histologic analysis of renal leukocyte infiltration in antineutrophil cytoplasmic antibody-associated vasculitis: Importance of monocyte and neutrophil infiltration in tissue damage. *Arthritis Rheum* 50: 3651–3657, 2004

29. Aasarød K, Bostad L, Hammerstrøm J, Jørstad S, Iversen BM: Wegener's granulomatosis: Inflammatory cells and markers of repair and fibrosis in renal biopsies—a clinicopathological study. *Scand J Urol Nephrol* 35: 401–410, 2001

30. Fiore N, Castellano G, Blasi A, Capobianco C, Loverre A, Montinaro V, Netti S, Torres D, Manno C, Grandaliano G, Ranieri E, Schena FP, Gesualdo L: Immature myeloid and plasmacytoid dendritic cells infiltrate renal tubulointerstitium in patients with lupus nephritis. *Mol Immunol* 45: 259–265, 2008

31. Castellano G, Trouw LA, Fiore N, Daha MR, Schena FP, van Kooten C: Infiltrating dendritic cells contribute to local synthesis of C1q in murine and human lupus nephritis. *Mol Immunol* 47: 2129–2137, 2010

32. Steinmetz OM, Velden J, Kneissler U, Marx M, Klein A, Helmchen U, Stahl RA, Panzer U: Analysis and classification of B-cell infiltrates in lupus and ANCA-associated nephritis. *Kidney Int* 74: 448–457, 2008

33. Snelgrove SL, Kausman JY, Lo C, Lo C, Ooi JD, Coates PT, Hickey MJ, Holdsworth SR, Kurts C, Engel DR, Kitching AR: Renal dendritic cells adopt a pro-inflammatory phenotype in obstructive uropathy to activate T cells but do not directly contribute to fibrosis. *Am J Pathol* 180: 91–103, 2012

34. van der Voort R, Kramer M, Lindhout E, Torensma R, Eleveld D, van Lieshout AW, Looman M, Ruers T, Radstake TR, Figdor CG, Adema GJ: Novel monoclonal antibodies detect elevated levels of the chemokine CCL18/DC-CK1 in serum and body fluids in pathological conditions. *J Leukoc Biol* 77: 739–747, 2005

35. Cai M, Bonella F, He X, Sixt SU, Sarria R, Guzman J, Costabel U: CCL18 in serum, BAL fluid and alveolar macrophage culture supernatant in interstitial lung diseases. *Respir Med* 107: 1444–1452, 2013

36. Tsicopoulos A, Chang Y, Ait Yahia S, de Nadai P, Chenivesse C: Role of CCL18 in asthma and lung immunity. *Clin Exp Allergy* 43: 716–722, 2013

37. Prasse A, Probst C, Bargagli E, Zissel G, Toews GB, Flaherty KR, Olschewski M, Rottoli P, Müller-Quernheim J: Serum CC-chemokine ligand 18 concentration predicts outcome in idiopathic pulmonary fibrosis. *Am J Respir Crit Care Med* 179: 717–723, 2009

38. Günther C, Zimmermann N, Berndt N, Grosser M, Stein A, Koch A, Meurer M: Up-regulation of the chemokine CCL18 by macrophages is a potential immunomodulatory pathway in cutaneous T-cell lymphoma. *Am J Pathol* 179: 1434–1442, 2011

39. Miyagaki T, Sugaya M, Suga H, Ohmatsu H, Fujita H, Asano Y, Tada Y, Kadono T, Sato S: Increased CCL18 expression in patients with cutaneous T-cell lymphoma: Association with disease severity and prognosis. *J Eur Acad Dermatol Venereol* 27: e60–e67, 2013

40. Chen J, Yao Y, Gong C, Yu F, Su S, Chen J, Liu B, Deng H, Wang F, Lin L, Yao H, Su F, Anderson KS, Liu Q, Ewen ME, Yao X, Song E: CCL18 from tumor-associated macrophages promotes breast cancer metastasis via PITPNM3. *Cancer Cell* 19: 541–555, 2011

41. Lindhout E, Vissers JL, Hartgers FC, Huijbens RJ, Scharenborg NM, Figdor CG, Adema GJ: The dendritic cell-specific CC-chemokine DC-CK1 is expressed by germinal center dendritic cells and attracts CD38-negative mantle zone B lymphocytes. *J Immunol* 166: 3284–3289, 2001

42. Hieshima K, Imai T, Baba M, Shoudai K, Ishizuka K, Nakagawa T, Tsuruta J, Takeya M, Sakaki Y, Takatsuki K, Miura R, Opdenakker G, Van Damme J, Yoshie O, Nomiyama H: A novel human CC chemokine PARC that is most homologous to macrophage-inflammatory protein-1 alpha/LD78 alpha and chemotactic for T lymphocytes, but not for monocytes. *J Immunol* 159: 1140–1149, 1997

43. Adema GJ, Hartgers F, Verstraten R, de Vries E, Marland G, Menon S, Foster J, Xu Y, Nooyen P, McClanahan T, Bacon KB, Figdor CG: A dendritic-cell-derived C-C chemokine that preferentially attracts naive T cells. *Nature* 387: 713–717, 1997

44. D'Ambrosio D, Iellem A, Bonecchi R, Mazzeo D, Sozzani S, Mantovani A, Sinigaglia F: Selective up-regulation of chemokine receptors CCR4 and CCR8 upon activation of polarized human type 2 Th cells. *J Immunol* 161: 5111–5115, 1998

45. Wei L, Vahedi G, Sun HW, Watford WT, Takatori H, Ramos HL, Takahashi H, Liang J, Gutierrez-Cruz G, Zang C, Peng W, O'Shea JJ, Kanno Y: Discrete roles of STAT4 and STAT6 transcription factors in tuning epigenetic modifications and transcription during T helper cell differentiation. *Immunity* 32: 840–851, 2010

46. Jakubzick C, Tacke F, Llodra J, van Rooijen N, Randolph GJ: Modulation of dendritic cell trafficking to and from the airways. *J Immunol* 176: 3578–3584, 2006

47. Qu C, Edwards EW, Tacke F, Angeli V, Llodrá J, Sanchez-Schmitz G, Garin A, Haque NS, Peters W, van Rooijen N, Sanchez-Torres C, Bromberg J, Charo IF, Jung S, Lira SA, Randolph GJ: Role of CCR8 and other chemokine pathways in the migration of monocyte-derived dendritic cells to lymph nodes. *J Exp Med* 200: 1231–1241, 2004

48. Krebs CF, Kapffer S, Paust HJ, Schmidt T, Bennstein SB, Peters A, Stege G, Brix SR, Meyer-Schwesinger C, Müller RU, Turner JE, Steinmetz OM, Wolf G, Stahl RA, Panzer U: MicroRNA-155 drives TH17 immune response and tissue injury in experimental crescentic GN. *J Am Soc Nephrol* 24: 1955–1965, 2013

49. Solez K, Colvin RB, Racusen LC, Haas M, Sis B, Mengel M, Halloran PF, Baldwin W, Banfi G, Collins AB, Cosio F, David DS, Drachenberg C, Einecke G, Fogo AB, Gibson IW, Glotz D, Iskandar SS, Kraus E, Lerut E, Mannon RB, Mihatsch M, Nankivell BJ, Nickeleit V, Papadimitriou JC, Randhawa P, Regele H, Renaudin K, Roberts I, Seron D, Smith RN, Valente M: Banff 07 classification of renal allograft pathology: Updates and future directions. *Am J Transplant* 8: 753–760, 2008

50. Chensue SW, Lukacs NW, Yang TY, Shang X, Frait KA, Kunkel SL, Kung T, Wiekowski MT, Hedrick JA, Cook DN, Zingoni A, Narula SK, Zlotnik A, Barrat FJ, O'Garra A, Napolitano M, Lira SA: Aberrant in vivo T helper type 2 cell response and impaired eosinophil recruitment in CC chemokine receptor 8 knockout mice. *J Exp Med* 193: 573–584, 2001

51. Turner JE, Paust HJ, Steinmetz OM, Peters A, Riedel JH, Erhardt A, Wegscheid C, Velden J, Fehr S, Mittrücker HW, Tiegs G, Stahl RA, Panzer U: CCR6 recruits regulatory T cells and Th17 cells to the kidney in glomerulonephritis. *J Am Soc Nephrol* 21: 974–985, 2010

52. Disteldorf EM, Krebs CF, Paust HJ, Turner JE, Nouailles G, Tittel A, Meyer-Schwesinger C, Stege G, Brix SR, Velden J, Wiech T, Helmchen U, Steinmetz OM, Peters A, Bennstein SB, Kaffke A, Llanto C, Lira SA, Mittrücker HW, Stahl RAK, Kurts C, Kaufmann SH, Panzer U. CXCL5 drives neutrophil recruitment in TH17-mediated GN [published online ahead of print on June 5, 2014]. *J Am Soc Nephrol* doi.10.1681/ASN.2013101061

53. Turner JE, Krebs C, Tittel AP, Paust HJ, Meyer-Schwesinger C, Bennstein SB, Steinmetz OM, Prinz I, Magnus T, Korn T, Stahl RA, Kurts C, Panzer U: IL-17A production by renal γδ T cells promotes kidney injury in crescentic GN. *J Am Soc Nephrol* 23: 1486–1495, 2012

54. Heymann F, Hammerich L, Storch D, Bartneck M, Huss S, Rüsseler V, Gassler N, Lira SA, Luedde T, Trautwein C, Tacke F: Hepatic macrophage migration and differentiation critical for liver fibrosis is mediated by the chemokine receptor C-C motif chemokine receptor 8 in mice. *Hepatology* 55: 898–909, 2012

55. Irizarry RA, Bolstad BM, Collin F, Cope LM, Hobbs B, Speed TP: Summaries of Affymetrix GeneChip probe level data. *Nucleic Acids Res* 31: e15, 2003

56. Bolstad BM, Irizarry RA, Astrand M, Speed TP: A comparison of normalization methods for high density oligonucleotide array data based on variance and bias. *Bioinformatics* 19: 185–193, 2003